Sequence-Specific Recognition of MicroRNAs and Other Short Nucleic Acids with Solid-State Nanopores

By: Osama K. Zahid, Fanny Wang, Jan A. Ruzicka, Ethan W. Taylor, and Adam R. Hall

Osama K. Zahid, Fanny Wang, Jan A. Ruzicka, Ethan W. Taylor, and Adam R. Hall. Sequence-Specific Recognition of MicroRNAs and Other Short Nucleic Acids with Solid-State Nanopores. *Nano Letters*. 2016, 16, 3, 2033–2039 https://doi.org/10.1021/acs.nanolett.6b00001

Abstract:

The detection and quantification of short nucleic acid sequences has many potential applications in studying biological processes, monitoring disease initiation and progression, and evaluating environmental systems, but is challenging by nature. We present here an assay based on the solid-state nanopore platform for the identification of specific sequences in solution. We demonstrate that hybridization of a target nucleic acid with a synthetic probe molecule enables discrimination between duplex and single-stranded molecules with high efficacy. Our approach requires limited preparation of samples and yields an unambiguous translocation event rate enhancement that can be used to determine the presence and abundance of a single sequence within a background of nontarget oligonucleotides.

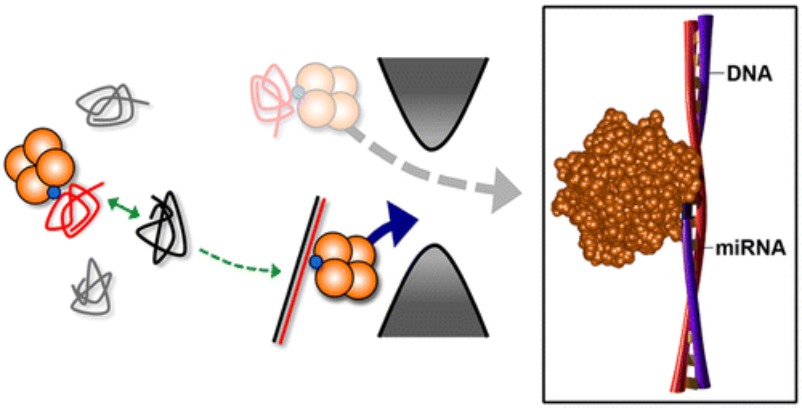

Keywords: Nanopore | sequence | microRNA | detection | cancer

Article:

The roles of short nucleic acid sequences are multiple and diverse. A prominent example is microRNA (miRNA), a family of 18–25 nt, noncoding RNAs that regulate a wide variety of cell functions and take part in post-transciptional silencing of genes.[1, 2] miRNAs are especially promising as biomarkers for cancer because anomalous levels have been identified in many tumor types.[3] In addition, they are known to exist as cell-free nucleic acids (cfNA) in serum and blood plasma,[4] making them potentially easy to collect through noninvasive means. However, such sequences present unique challenges for conventional detection technologies. For example, quantitative real-time PCR is prone to amplification errors,[5] while microarray assays require extensive design and labeling of probes or targets to be validated. As a result, new approaches are highly desirable.

We recently reported[6] a SS-nanopore approach for the selective detection of target DNA. In conventional SS-nanopore measurements, a nanometer-scale aperture formed in a thin membrane is positioned between two chambers of electrolyte solution and used for resistive pulse sensing of molecules as they thread electrically through it (Figure 1a). In our approach, a set of biomolecules is used that individually do not yield significant translocation signals (events): a monovalent variant of streptavidin[7] (MS) and a short, biotinylated double-stranded DNA (dsDNA). When the two bind, the construct yields a large increase in event rate that can be used for direct molecular quantification. Here, we apply this new assay to the high-fidelity detection of specific miRNAs and other short nucleic acid sequences in solution.

The mechanisms underlying our method are yet unestablished. It has been demonstrated that wild type streptavidin translocates rapidly[8] and is thus beyond the resolution of conventional electronics.[9] This is also true for the MS we use, which contains an additional hexaglutamate tag for isolation[10] and thus has a net charge of $-17.1e$, further increasing its electrophoretic velocity. However, the absence of events for short dsDNA, and thus the origin of the rate enhancement itself, is less clear. Our initial working hypothesis[6] was that nucleic acid attachment to the MS supplied an additional hydrodynamic drag to the fast-moving protein, thus slowing nucleoprotein translocation to a resolvable speed. However, this implied that the dsDNA itself experienced a net repulsive force, possibly caused by electroosmotic shear force counteracting electrophoresis. While translocation physics at this length scale is not fully characterized and experimental factors like solvent conditions and SS-nanopore surface charge can alter expected dynamics,[11] electrophoretic velocity and direction of motion are understood to be independent of length,[12] especially under high-salt conditions where the Debye layer is thin. In addition, a limited number of previous reports[13-16] have directly measured the translocation of short DNA through SS-nanopores, albeit under different experimental conditions. Together, these considerations suggest that short oligonucleotides indeed translocate under a positive bias, potentially making our initial interpretation unphysical.

An alternative hypothesis is that the short dsDNA translocations are also rapid and thus challenge bandwidth limitations, much like those of MS. In this case, the subsequent rate enhancement could arise from transient interactions[17] with the SS-nanopore walls, facilitated by the bulkier nucleoprotein complex and resulting in protracted and resolvable event durations. While we observe that our measurements are highly stable, with individual nanopores supporting thousands of events without clogging, this effect does appear to be at play. Nonetheless, other considerations are likely important as well. For example, capture of dsDNA of length <8000 bp

into a nanopore can be described well by an entropic barrier-limited model,[18, 19] dependent principally on molecular orientation, but also with weaker dependences on electrophoretic and conformational components. In the case of subpersistence length DNA, the conformational term is irrelevant. However, extending to our nucleoprotein complex, the dominant orientational factor (rotational hydrodynamics) will be perturbed by the bound MS, and the normally weak electrophoretic component may be influenced strongly by the significant charge of the protein, especially for very short DNA. These mechanistic details will be the subject of further studies.

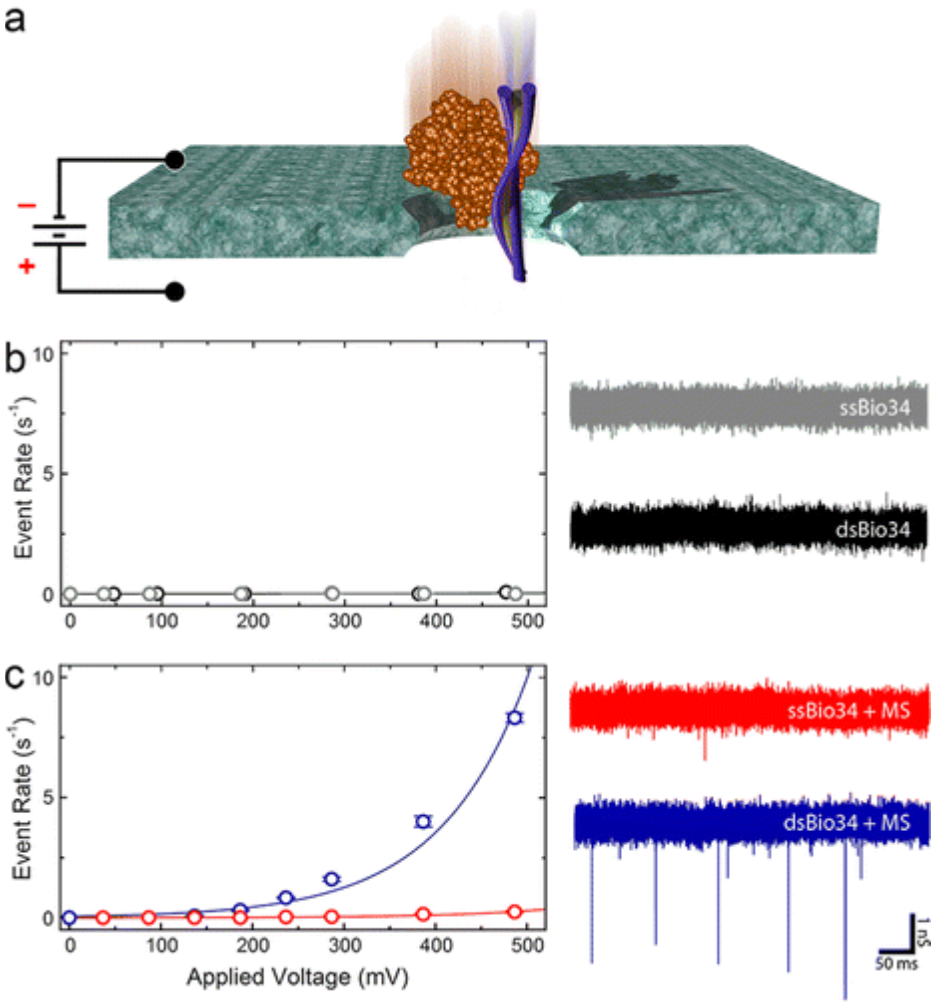

Figure 1. Selective detection of dsDNA. (a) Schematic showing a short duplex DNA molecule bound to MS translocating electrically through a SS-nanopore. (b) Event rate vs applied voltage for ssBio34 (gray) and dsBio34 (black) without MS bound (1 μM). Example transmembrane ionic current traces (colors matched) recorded at 500 mV are shown to the right. (c) Event rate vs applied voltage for ssBio34 (red) and dsBio34 (blue) with MS bound (1 μM). All solid lines are exponential fits to the data. Example traces (colors matched) recorded at 500 mV are shown to the right. Scale bar (lower right) applies to all traces.

Because our assay is able to selectively probe monobiotinylated dsDNA, we hypothesized that hybridization between target single-stranded (ss-) molecules, and complementary synthetic biotinylated oligonucleotides could be used to identify sequences in solution. However, such an approach would be possible only under the condition that biotinylated ssDNA itself does not produce events, either individually or in complex with MS. To investigate this, we focused on

two short DNA constructs (see Table S1): a 34 nt ssDNA containing a single biotin moiety (ssBio34) and the same oligonucleotide hybridized to its (nonbiotinylated) complementary sequence to form 34 bp dsDNA (dsBio34). When introduced to a SS-nanopore independently, neither molecule yielded translocation events (Figure 1b). Next, we repeated the measurements following incubation of each molecule with an excess of MS to form nucleoprotein complexes. For the ssBio34:MS, we again observed very few events across the entire investigated voltage range (Figure 1c, red); for example, the rate at 500 mV was only 0.24 s^{-1}. However, under identical conditions, dsBio34:MS yielded a dramatic increase in translocation event rate that scaled exponentially[19] with applied voltage (Figure 1c, blue). For voltages above 200 mV, the rate was greater than an order of magnitude higher than that of ssBio34:MS. The mean depth and duration of events (Figure 2) at lower voltages showed a single, deep (2.5–3 nS) blockade level and translocation durations at or below the temporal resolution of our system, similar to our previous report with 90 bp dsDNA.[6] As voltage was increased further, however, we observed the emergence of a bimodal distribution. This behavior is likely caused by the occurrence of both translocation and collision events brought on by two discrete modes of molecular orientation during translocation[20] and made resolvable by the increased signal-to-noise ratio at high voltage. Regardless of the explanation, these experiments demonstrated the viability of sequence detection.

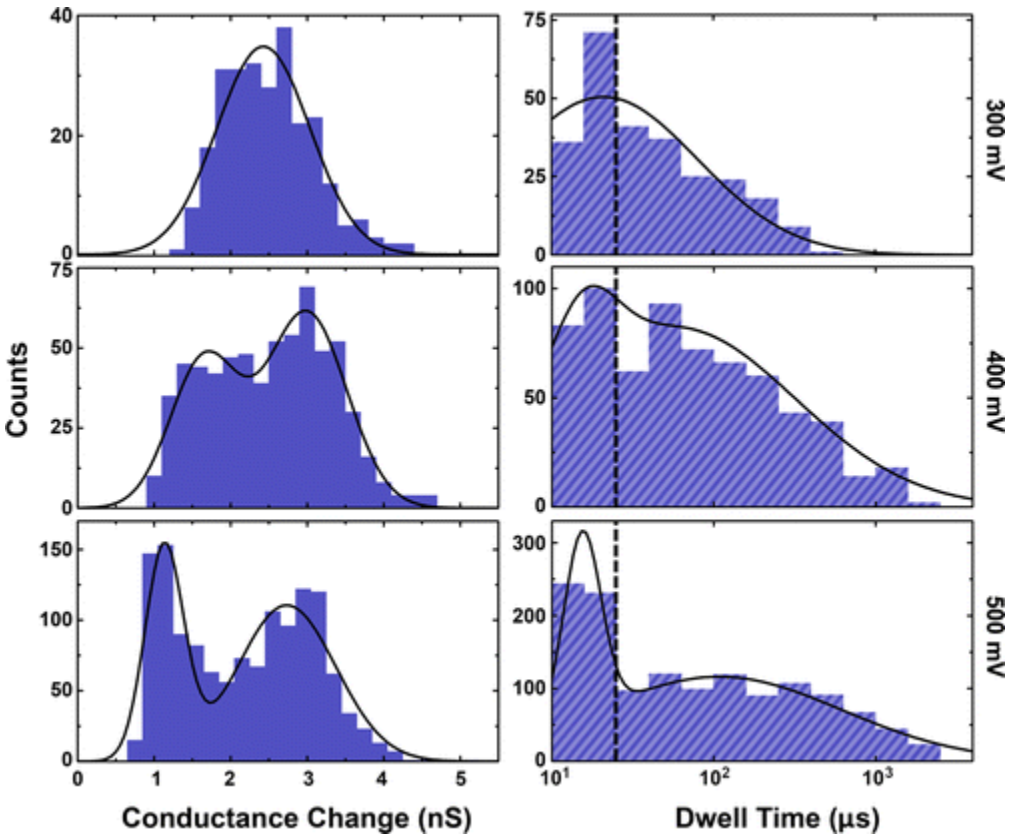

Figure 2. Analysis of dsDNA:MS events. Event depth (left) and duration (right) histograms of dsDNA:MS (1 µM) from 300 (top) to 500 mV (bottom). Solid lines are Gaussian fits to the data, and the dashed line represents the temporal resolution of our system. Number of events represented are (T-B) 262, 652, and 1332, respectively.

We next utilized our approach to recognize a specific sequence within a heterogeneous mixture (Figure 3). Here, we used ssBio34 as a "bait" sequence; by incubating it with a mixture of ssDNA, dsBio34 could be formed only if its complement (the "target" sequence) was present. To test this, we first prepared a mixture of three unlabeled ssDNA oligonucleotides (see Table S1) with low (~25%) homology to the bait or target to act as nonspecific decoy sequences. Combining these decoys with target sequence, performing a single thermal cycle to promote annealing, and incubating with an excess of MS yielded no significant SS-nanopore translocation events (Figure 3b, black). This followed our expectations since presumably only nonbiotinylated ssDNA molecules were present. An identical protocol with background sequences and ssBio34 bait similarly produced very few events (Figure 3b, red) because dsBio34 is absent. We did observe a minor increase in capture rate as compared to ssDNA alone or to ssBio34:MS alone, which we attributed to partial hybridization; intrastrand complexes may be sufficiently large to promote minor rate enhancement. It is likely that this effect could be minimized through manipulation of experimental conditions like solvent temperature to discourage low-energy hybridization.

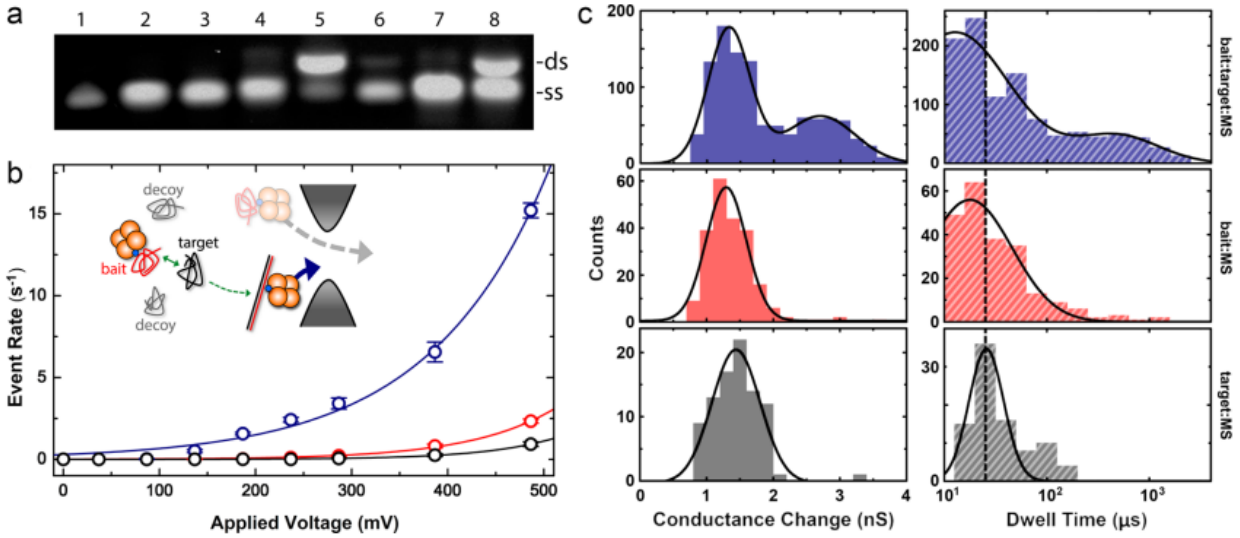

Figure 3. Sequence selection within a mixture. (a) Agarose gel electrophoresis analysis of bait (lane 1), decoys 1–3 (lanes 2–4), bait/target (equimolar ratio, lane 5), target (lane 6), bait/decoys (lane 7), and bait/target/decoys (equimolar ratio, lane 8). ds and ss denote double- and single-stranded oligonucleotides, respectively. (b) Event rate vs applied voltage for the target sequence (nonbiotinylated complement to ssBio34, black), the bait sequence (ssBio34, red), and both the bait and target sequences (blue). All mixtures were incubated with MS among a background of three noncomplementary decoy oligonucleotides. All molecules were supplied at a concentration of 1 μM. Solid lines are exponential fits to the data. Inset: schematic of sequence selection detection. (c) Mean event depth (left) and dwell time (right) histograms for each sample (colors match (b)). Solid lines are Gaussian fits to the data, and the dashed line represents the temporal resolution of our system. Note that a second peak in the red and gray data sets could not be reliably fit due to the insignificant number of deep and long events. Total number of events considered are (T-B) 1080, 223, and 89, respectively.

When bait, target, and background sequences were coannealed and incubated with MS, the resulting mixture again produced a large increase in the number of recorded events (Figure 3b, blue). Although the number of translocation events generated by bait/decoys/MS was not insignificant, bait/target coupling was marked by a relative enhancement of about an order of magnitude under applied voltages of >150 mV. Consequently, this result demonstrated that our assay could be used to discriminate a single sequence of interest from a heterogeneous mixture

with high specificity. We note that the event rate for bait/target/MS among background sequences was somewhat higher than was observed for the same concentration of dsBio34:MS alone (Figure 1c). This may be caused by both the intrastrand interactions described above and minor pore-to-pore variations (e.g., local charge density or diameter). Figure 3c shows a representative set of event depth and duration histograms for the three samples, collected at 500 mV. For the bait/target/MS sample, we found a bimodal distribution, similar to the high-voltage data in Figure 2. We again attribute this to the occurrence of both translocation and collision events. For the control samples, we observed a single, Gaussian distribution in both values, with most events occurring at or below the temporal resolution of our instrument. This suggests that the population to the right in each histogram (high conductance change and long duration) represents collisions since they are far more prevalent for the larger nucleoprotein complex; only a few bait/decoy/MS events (<1%) fall within the same range. This distribution disparity may offer an additional metric by which to confirm detection of target sequences.

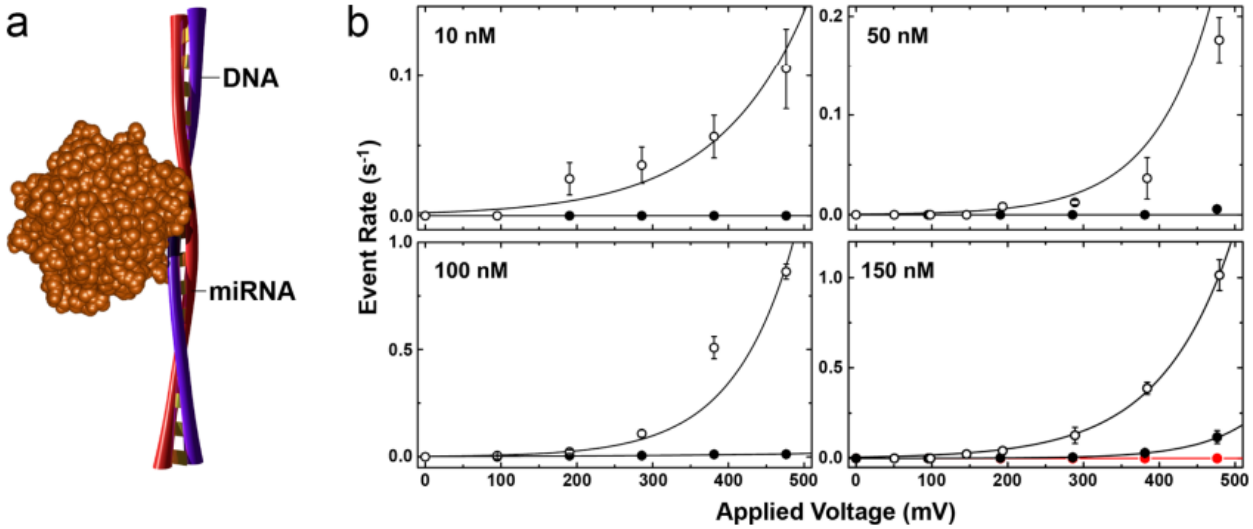

Figure 4. miRNA detection. (a) Schematic of monobiotinylated ssDNA bait oligonucleotide (blue) annealed to target miR155 ssRNA (red) to form a 23 bp DNA–RNA heteroduplex with bound MS (orange). (b) Typical plots of event rate vs applied voltage for ssBio23:MS (closed circles) and ssBio23:miR155:MS (open circles), at 10, 50, 100, and 150 nM, respectively. The red data points in the 150 nM plot are measurements of miR155 alone. Solid lines are exponential fits to the data.

Having established the ability of the assay to selectively detect a target sequence, we finally demonstrated that the approach could be used to detect a specific miRNA. We used as a demonstration vehicle the miRNA designated hsa-mi-R155 (miR155), a 23 nt ssRNA that is an established biomarker of lung cancer.[21, 22] To accomplish miRNA sequence detection, we employed a ssDNA bait construct (ssBio23, see Table S1) with a single internal biotin and complementarity to the miR155 sequence (Supplementary Figure S1). When ssBio23 was annealed with miR155 target to form a DNA–RNA heteroduplex (Figure 4a), we observed an enhanced voltage-dependent event rate across a range of concentrations (Figure 4b). As before, measurements with ssBio23, either alone or incubated with a molar excess of MS, yielded few events under all investigated conditions. Unsurprisingly, the same was true of the miR155 alone (Figure 4b, red). Event rate for the heteroduplex bound by MS was found to vary linearly with concentration for several voltages (Figure 5a), in agreement with previous SS-nanopore measurements of short nucleic acids.[13] Analysis of mean event depth and duration (Figure 5b)

showed less striking bimodal distributions than for the 34 bp constructs described above, likely due to the significantly smaller size of these molecules. Notably, the rate enhancement was sufficient to detect with high resolution as little as 10 nM ssBio23:miR155 heteroduplex, within the range of physiological miR155 concentrations,[23] for example. Collectively, these results confirmed both the viability of our assay down to the length scale of 23 nt as well as its applicability to RNA targets and suggests its potential clinical utility.

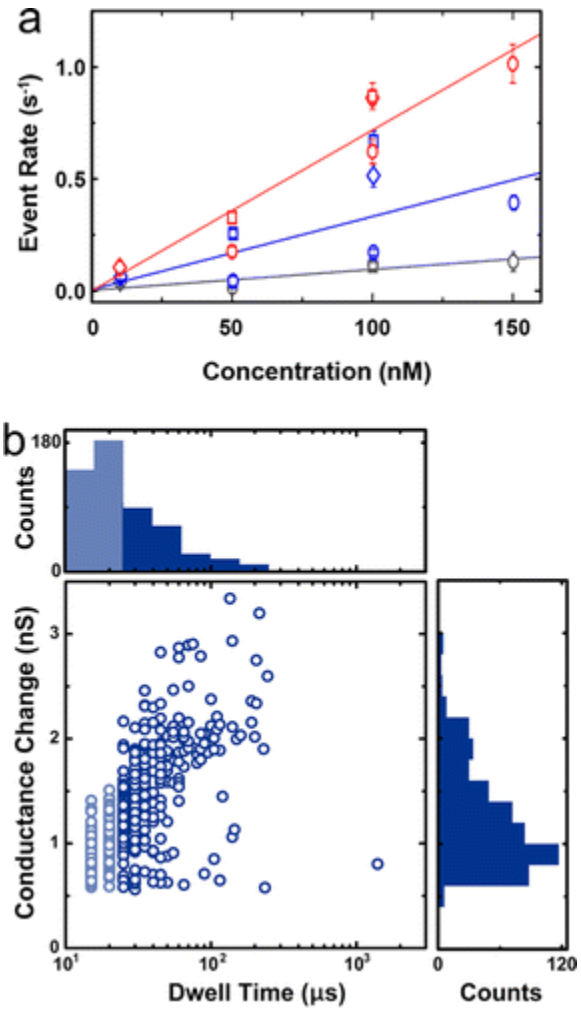

Figure 5. miRNA heteroduplex analyses. (a) Event rate vs concentration for ssbio23:miR155 heteroduplex with bound MS at applied voltages of 300 (gray), 400 (blue), and 500 (red). Different symbols represent data collected from different individual pores. Solid lines are linear fits to the data. (b) Scatter plot and accompanying histograms of mean event depth (conductance change) and duration (dwell time) for ssBio23:miR155:MS at 500 mV. Faded region (left) represents events below the temporal resolution of the system.

There have been only two prior reports of miRNA analysis with nanopore systems. Wanunu et al. pioneered SS-nanopore detection of miRNA, enabled by the use of ultrathin membranes.[13] They used their system to distinguish a single miRNA in rat liver extract. However, the approach required significant sample purification and concentration of miRNA target due to the nonselective nature of conventional SS-nanopore detection. A distinct difference between this and the present work is that our approach can resolve target sequences from among a background of ancillary molecules, potentially removing the need for extensive enrichment of the target

sequence. Wang et al. demonstrated sequence-specific detection of miRNA with the α-hemolysin protein nanopore,[23] using the method to distinguish miR155 in patient serum. This important approach yielded information that is qualitatively similar to our results. However, the techniques differ in two key respects. First, the α-hemolysin system is built on lipid bilayers that are still challenging to integrate into stable device architectures, despite recent commercial progress.[24] Our system is built on silicon-based materials, which could promote easier integration and parallelization. Second, the previous measurement relied on differentiation between signals produced by target molecules as well as other background sequences, thus requiring some degree of thresholding and selection in analysis. In contrast, the present approach produces an unambiguous signal, essentially only yielding events when target sequences are present.

In conclusion, we have reported a SS-nanopore approach that uses hybridization with a biotinylated oligonucleotide to identify short nucleic acid sequences, including miRNA. The measurement is rapid and amenable to integration in wafer-scale device architectures. We first demonstrated that dsDNA could be differentiated from ssDNA with high fidelity and subsequently that a single target sequence could be detected selectively. Indeed, identification from among a mixture of similarly sized, noncomplementary ssDNA was marked by a rate enhancement of more than an order of magnitude. Finally, we applied the technique to the *in vitro* sensing of a specific miRNA, miR155, that has importance as a lung cancer biomarker. We demonstrated detection of as little as 10 nM miRNA, validating the detection of physiologically relevant concentrations.[25] We believe this resolution could be improved through the use of salt gradients[19, 23] or further optimization of device dimensions, for example. This embodiment of SS-nanopore detection enables selectivity for arbitrary nucleic acid sequences and thus could be valuable for the sensitive analysis of biomarkers of disease,[26] contamination,[27] and bioterrorism agents.[28]

Materials and Methods

Biomolecule Preparation

All synthetic nucleic acids, including 34 nt biotinylated (bait) and nonbiotinylated (target) ssDNA, low-homology background sequences, 23 nt biotinylated (bait) ssDNA, and 23 nt miR155 (target) ssRNA, were obtained commercially (Integrated DNA Technologies, Coralville, IA). Sequences are provided in Supplementary Table S1. All ssDNA molecules were resuspended in pure deionized water (Milli-Q) to a stock concentration of 200 μM and stored at −20 °C prior to use. miR155 was aliquoted out in clean eppendorf tubes and stored to prevent contamination and degradation. Complementary oligonucleotides were hybridized by incubating the samples at a 1:1 molar ratio in pure deionized water at 95 °C for 10 min and gradually cooling to room temperature to generate duplex material (dsBio34 or 23 bp heteroduplex) at a final concentration of 8 μM, as confirmed by spectrophotometry. Hybridization was confirmed by gel electrophoresis. An identical hybridization reaction was conducted in the presence of three decoy ssDNA oligonucleotides (42, 40, and 33 bps in length, respectively) for the selectivity measurement. Constructs were validated on a 4% agarose gel prepared in 1× TBE buffer with GelRed nucleic acid stain (Phenix Research Products, Candler, NC). Gel images were captured using a Gel Doc system (BioRad, Hercules, CA).

Binding Reaction Incubation

MS, a 54.5 kDa streptavidin variant (SAe1D3) that contains one active biotin-binding site,[7] was supplied by the Howarth lab (Oxford University). The protein contains a covalent hexaglutamate tag[10] used for isolation that imparts a net charge of −17.1*e* under pH conditions comparable to those used here. For all experiments, 2.5 μL of prepared oligonucleotides at a stock concentration of 8 μM was incubated with 1 μL of MS (50 μM stock) in 1× PBS at room temperature for 10 min and brought to a final salt concentration of 900 mM NaCl and 0.5× PBS. The resulting mixture contained 1 μM DNA and a 2.5× molar excess of MS. When necessary, further dilutions were performed using measurement buffer.

Nanopore Fabrication, Detection, and Analysis

Silicon chips (4.4 mm) containing 25 nm thick, free-standing silicon nitride membranes were obtained commercially (Norcada, Inc., Alberta, Canada). In each membrane, an individual nanopore (diameter 7.5–9.0 nm) was fabricated using a scanning helium ion microscope (Carl Zeiss Orion Plus) technique described elsewhere.[29] Nanopore chips were stored in a 50% ethanol solution until use. Directly before measurement, a chip was rinsed with deionized water and ethanol, dried under filtered air flow, and then exposed to air plasma (30 W) for 2 min on each side before being placed into a custom Ultem 1000 flow cell and immediately introduced with measurement buffer on both sides. A patch clamp amplifier (Axopatch 200B) was used to apply voltage and record current through Ag/AgCl electrodes. Each device was verified to exhibit a steady baseline and linear current vs voltage characteristics that corresponded to intended pore diameter.[30] Current traces were collected at a rate of 200 kHz with a 100 kHz four-pole Bessel filter and analyzed with custom software, through which an additional 25 kHz low-pass filter was applied to all data. Devices were stable throughout the measurements, typically supporting >4000 events. An event was defined as having amplitude above a threshold of 4.5σ and duration between 12.5 to 1200 μs. Rate was determined by analyzing for each voltage an uninterrupted current trace of either 150 s (for 34 bp data sets) or 370–740 s (for 23 bp data sets). Data was saved in increments of 3.2 s, and the standard deviation of the rates was used as measurement error. DNA measurements were performed in triplicate. We display typical results from a single nanopore for consistency and to avoid effects of pore-to-pore variation. Additional data is presented in Figure S2 to demonstrate the repeatability of the measurement.

Supporting Information

The Supporting Information is available at https://doi.org/10.1021/acs.nanolett.6b00001.

Notes

(J.A.R.) School of Pharmacy, High Point University, High Point, North Carolina 27268, United States.

The authors declare the following competing financial interest(s): A.R.H. is listed as inventor on a patent covering the presented SS-nanopore assay for sequence detection.

Acknowledgment

The authors thank the Howarth lab (Oxford University) for supplying monovalent streptavidin and F. Perrino and S. Harvey (Wake Forest School of Medicine) for assistance with RNA handling. This work was supported by NIH grant 1R21CA193067. E.W.T. and J.A.R. acknowledge funding from The Dr. Arthur and Bonnie Ennis Foundation, Decatur, IL. A.R.H. acknowledges support from the 3M Nontenured Faculty Award program.

References

1. He, L.; Hannon, G. J. MicroRNAs: small RNAs with a big role in gene regulation Nat. Rev. Genet. **2004**, 5, 522– 531 DOI: 10.1038/nrg1379 Google Scholar
2. Carthew, R. W.; Sontheimer, E. J. Origins and Mechanisms of miRNAs and siRNAs Cell **2009**, 136, 642– 655 DOI: 10.1016/j.cell.2009.01.035 Google Scholar
3. Lu, J.MicroRNA expression profiles classify human cancers Nature **2005**, 435, 834– 838 DOI: 10.1038/nature03702 Google Scholar
4. Mitchell, P. S.Circulating microRNAs as stable blood-based markers for cancer detection Proc. Natl. Acad. Sci. U. S. A. **2008**, 105, 10513– 10518 DOI: 10.1073/pnas.0804549105 Google Scholar
5. Ruijter, J. M.Amplification efficiency: linking baseline and bias in the analysis of quantitative PCR data Nucleic Acids Res. **2009**, 37, e45 DOI: 10.1093/nar/gkp045 Google Scholar
6. Carlsen, A. T.; Zahid, O. K.; Ruzicka, J. A.; Taylor, E. W.; Hall, A. R. Selective detection and quantification of modified DNA with solid-state nanopores Nano Lett. **2014**, 14, 5488– 5492 DOI: 10.1021/nl501340d Google Scholar
7. Howarth, M.A monovalent streptavidin with a single femtomolar biotin binding site Nat. Methods **2006**, 3, 267– 273 DOI: 10.1038/nmeth861 Google Scholar
8. Plesa, C.Fast Translocation of Proteins through Solid State Nanopores Nano Lett. **2013**, 13, 658– 663 DOI: 10.1021/nl3042678 Google Scholar
9. Larkin, J.; Henley, R. Y.; Muthukumar, M.; Rosenstein, J. K.; Wanunu, M. High-Bandwidth Protein Analysis Using Solid-State Nanopores Biophys. J. **2014**, 106, 696– 704 DOI: 10.1016/j.bpj.2013.12.025 Google Scholar
10. Fairhead, M.; Krndija, D.; Lowe, E. D.; Howarth, M. Plug-and-Play Pairing via Defined Divalent Streptavidins J. Mol. Biol. **2014**, 426, 199– 214 DOI: 10.1016/j.jmb.2013.09.016 Google Scholar
11. Firnkes, M.; Pedone, D.; Knezevic, J.; Doeblinger, M.; Rant, U. Electrically facilitated translocations of proteins through Silicon Nitride nanopores: conjoint and competitive action of diffusion, electrophoresis, and electroosmosis Nano Lett. **2010**, 10, 2162– 2167 DOI: 10.1021/nl100861c Google Scholar

12. Viovy, J.-L. Electrophoresis of DNA and other polyelectrolytes: Physical mechanisms Rev. Mod. Phys. **2000**, 72, 813– 872 DOI: 10.1103/RevModPhys.72.813 Google Scholar

13. Wanunu, M.Rapid electronic detection of probe-specific microRNAs using thin nanopore sensors Nat. Nanotechnol. **2010**, 5, 807– 814 DOI: 10.1038/nnano.2010.202 Google Scholar

14. Rosenstein, J. K.; Wanunu, M.; Merchant, C. A.; Drndic, M.; Shepard, K. L. Integrated nanopore sensing platform with sub-microsecond temporal resolution Nat. Methods **2012**, 9, 487– U112 DOI: 10.1038/nmeth.1932 Google Scholar

15. Venta, K.Differentiation of Short, Single-Stranded DNA Homopolymers in Solid-State Nanopores ACS Nano **2013**, 7, 4629– 4636 DOI: 10.1021/nn4014388 Google Scholar

16. Lee, M.-H.A Low-Noise Solid-State Nanopore Platform Based on a Highly Insulating Substrate Sci. Rep. **2014**, 4, 7448 DOI: 10.1038/srep07448 Google Scholar

17. Wanunu, M.; Sutin, J.; McNally, B.; Chow, A.; Meller, A. DNA translocation governed by interactions with solid-state nanopores Biophys. J. **2008**, 95, 4716– 4725 DOI: 10.1529/biophysj.108.140475 Google Scholar

18. Rowghanian, P.; Grosberg, A. Y. Electrophoretic capture of a DNA chain into a nanopore Phys. Rev. E **2013**, 87, 042722 DOI: 10.1103/PhysRevE.87.042722 Google Scholar

19. Wanunu, M.; Morrison, W.; Rabin, Y.; Grosberg, A. Y.; Meller, A. Electrostatic focusing of unlabelled DNA into nanoscale pores using a salt gradient Nat. Nanotechnol. **2010**, 5, 160– 165 DOI: 10.1038/nnano.2009.379 Google Scholar

20. Carlsen, A. T.; Zahid, O. K.; Ruzicka, J.; Taylor, E. W.; Hall, A. R. Interpreting the Conductance Blockades of DNA Translocations through Solid-State Nanopores ACS Nano **2014**, 8, 4754– 4760 DOI: 10.1021/nn501694n Google Scholar

21. Yanaihara, N.Unique microRNA molecular profiles in lung cancer diagnosis and prognosis Cancer Cell **2006**, 9, 189– 198 DOI: 10.1016/j.ccr.2006.01.025 Google Scholar

22. Donnem, T.Prognostic impact of MiR-155 in non-small cell lung cancer evaluated by in situ hybridization J. Transl. Med. **2011**, 9, 6 DOI: 10.1186/1479-5876-9-6 Google Scholar

23. Wang, Y.; Zheng, D.; Tan, Q.; Wang, M. X.; Gu, L.-Q. Nanopore-based detection of circulating microRNAs in lung cancer patients Nat. Nanotechnol. **2011**, 6, 668– 674 DOI: 10.1038/nnano.2011.147 Google Scholar

24. Ip, C. L. C.MinION Analysis and Reference Consortium: Phase 1 data release and analysis F1000Research **2015**, DOI: 10.12688/f1000research.7201.1 Google Scholar

25. Schmittgen, T. D.Real-time PCR quantification of precursor and mature microRNA Methods **2008**, 44, 31– 38 DOI: 10.1016/j.ymeth.2007.09.006 Google Scholar

26. Chen, X.Characterization of microRNAs in serum: a novel class of biomarkers for diagnosis of cancer and other diseases Cell Res. **2008**, 18, 997– 1006 DOI: 10.1038/cr.2008.282 Google Scholar

27. Greisen, K.; Loeffelholz, M.; Purohit, A.; Leong, D. Pcr Primers and Probes for the 16s Ribosomal-Rna Gene of Most Species of Pathogenic Bacteria, Including Bacteria Found in Cerebrospinal-Fluid J. Clin. Microbiol. **1994**, 32, 335– 351 Google Scholar

28. Lim, D. V.; Simpson, J. M.; Kearns, E. A.; Kramer, M. F. Current and developing technologies for monitoring agents of bioterrorism and biowarfare Clin. Microbiol. Rev. **2005**, 18, 583– 607 DOI: 10.1128/CMR.18.4.583-607.2005 Google Scholar

29. Yang, J. Rapid and precise scanning helium ion microscope milling of solid-state nanopores for biomolecule detection Nanotechnology **2011**, 22, 285310 DOI: 10.1088/0957-4484/22/28/285310 Google Scholar

30. Smeets, R. M. M.Salt dependence of ion transport and DNA translocation through solid-state nanopores Nano Lett. **2006**, 6, 89– 95 DOI: 10.1021/nl052107w Google Scholar

31. Wanunu, M.; Morrison, W.; Rabin, Y.; Grosberg, A. Y.; Meller, A. Electrostatic focusing of unlabelled DNA into nanoscale pores using a salt gradient Nat. Nanotechnol. **2010**, 5, 160– 165 DOI: 10.1038/nnano.2009.379 Google Scholar